Synthesis, and characterization of chitosan bearing pyranoquinolinone moiety for textile dye adsorption from wastewater

Shaimaa M. Ibrahim, Hany M. Hassanin and Marwa M. Abdelrazek

ABSTRACT

A novel compound was synthesized by the reaction of the amino group of the chitosan with the formyl group of pyrano[3,2-c]quinoline-3-carboxaldehyde moiety, which produced chitosan modified with a Schiff base (chitosan Schiff base). The structure of the newly prepared composite was elucidated. Chitosan Schiff base was used to remove the textile anionic remazol red (RR) dye from wastewater. The kinetic data and adsorption isotherm were best fitted by the pseudo-second-order kinetic model and the Freundlich isotherm, respectively. Thermodynamic parameters were calculated. Chitosan Schiff base resulted in 100% removal of carcinogenic dye at 2 min only with q_m 344.8 mg/g, and may do the same for other anionic reactive dyes, thus avoiding secondary pollution.

Key words | adsorption, anionic dye, chitosan, pyranoquinolinone, Schiff base, triethylorthoformate

Shaimaa M. Ibrahim (corresponding author)
Hany M. Hassanin
Marwa M. Abdelrazek
Department of Chemistry, Faculty of Education,
Ain Shams University,
Cairo,
Egypt
E-mail: *shimaaabdelaal@edu.asu.edu.eg*

INTRODUCTION

Chitosan is known to be the most plentiful and low cost biopolymer in nature; it forms most of the exoskeleton of crustaceans. Chitosan, or poly-(1, 4)-2-amino-2-deoxy-b-D-glucose, has many medical, pharmaceutical, and agricultural uses because it is a nontoxic (Zivanovic *et al.* 2007), heterogeneous, linear, cationic biocompatible, and biodegradable polysaccharide with a high molecular weight (El-Harby *et al.* 2017). By comparison with other polysaccharides, it contains about 6.9% nitrogen, which works as a chelating agent, so it is widely used in the pharmaceutical, biomedical, drug release and wound healing fields and in other applications. The unique structure of chitosan is due to the presence of active amino ($-NH_2$) and hydroxyl (–OH) groups, which are reactive adsorption sites for many organic and inorganic water pollutants (Saud *et al.* 2019). A free $-NH_2$ group results from the deacetylation of chitin, which helps in the modification of chitosan to produce different Schiff bases by reacting with several aldehydes and ketones (Manimohan *et al.* 2019).

Recently, chitosan derivatives have received great attention for promising applications in water and wastewater treatment technology (Saud *et al.* 2019). Modifying chitosan can be carried out easily using chemical or physical methods to produce chitosan derivatives with new functional groups. These methods may be used to improve its adsorption capacity or adsorption kinetics, enhancing the affinity of the sorbent and changing the selectivity of sorption (Tanhaei *et al.* 2016).

Schiff bases are considered one of the most important modifications for chitosan (Salama *et al.* 2015). These substances are used for analytical and environmental applications. There are many reports of the synthesis of Schiff bases of chitosan and their evaluation as adsorbents for dye removal. In addition, the additional N center inserted in chitosan Schiff base formation is expected to increase the adsorption capacity of chitosan towards anionic dyes by electrostatic interaction with protonated N centers (Manchaiah & Badalamoole. 2019).

Despite the presence of a large number of chitosan Schiff bases with different aldehydes (Nuriye *et al.* 2012; Salama *et al.* 2015; Elbadawy 2016), there is no research on a chitosan Schiff base incorporating a pyranoquinolinone moiety. Pyranoquinolinone (4-hydroxy-6-methyl-2,5-dioxo-5,6-dihydro-2H-pyrano[3,2c]quinoline-3-carboxaldehyde) is a very important compound in natural products and this moiety has shown antimalarial, HIV inhibitor, pharmaceutical, antischistosomal, antimicrobial and antitumor activity (Swathi *et al.* 2016). It is expected that the modification of chitosan with pyranoquinolinone may enhance

doi: 10.2166/wst.2020.097

some of the physical properties and antimicrobial activity of chitosan (Salama *et al.* 2015).

Industrial dye waste water, which is produced from the textile printing and dyeing industries, and from the production of food, paper, plastics and other products, results in serious health and environmental pollution due to its noticeably bright color, high toxicity and difficult degradation process. Most organic dyes are teratogenic, carcinogenic and mutagenic to human and marine life because of the presence of aromatic rings in their structure. There are also the problems of low degradability, high toxicity, and high stability to photo-degradation (Huanhuan *et al.* 2018; Ahmed *et al.* 2019). Hence, the treatment of these effluents is challenging (Manchaiah & Badalamoole 2019).

Many processes are used to purify wastewater containing dyes, but, most of these processes need appropriate conditions and have high operational costs (Amtul *et al.* 2018). Adsorption has been found to be very promising for removing textile dyes from wastewater (Geyse *et al.* 2017). Adsorption is an effective separation technique that is cost effective, simple, efficient, and non-reactive towards toxic agents (Amtul *et al.* 2018). Activated carbon is the most commonly used substance for dye removal by adsorption, although performance is dependent on the type of carbon used, its cost (Ukanwa *et al.* 2019), the characteristics of the wastewater, and the type of dye. So, the industry requires highly effective, low-cost adsorbents that are available in tonnage quantities, and do not present an environmental problem themselves (Blackburn 2004). Nowadays, there is an increasing requirement for novel polymers in industrial sectors for the effective elimination of dyes (Amtul *et al.* 2018). Chitosan is considered to be an active substance for the sorption of organic compounds such as phenols, metal ions, biphenyls, polychlorinated biphenyls, and proteins compared to other polymers. This is due to the presence of hydroxyl and amino groups on the polymer chains that act as the coordination and electrostatic interaction centers.

Traditionally, when chitosan has been directly used in the purification of water, it is mostly efficient in adsorbing negatively charged dyes in acidic conditions as a result of protonated amine groups. Chitosan has been used as a green cross linker, taking advantage of its amine groups as functional moieties participating in the formation of covalent bonds (Yang *et al.* 2016). Currently, many researchers are aiming to modify applied adsorbents to have multiple advantages such as industrial practicality, low cost, high removal rates, and (in some cases) recovery of the species involved without losing their chemical identity to be effective adsorbents in the purification of wastewater (Wan Ngaha *et al.* 2011; Geyse *et al.* 2017). Chitosan has been modified to prevent dissolution as well as to enhance the mechanical resistance and reinforcement of the chemical stability of chitosan in acidic solutions. These properties are important in an effective adsorbent (El-Harby *et al.* 2017).

So, the aim of present work was to study the ability of chitosan Schiff base for the removal of remazol red (RR; RB-133) dye, and compare this efficiency in absorbing dyes with other modified chitosan polymers. This was followed by the characterization of chitosan Schiff base using Fourier transform infrared spectroscopy (FT-IR), X-ray diffraction (XRD), scanning electron microscopy (SEM) and thermogravimetric analysis (TGA). In addition, kinetic and isotherm models were studied.

EXPERIMENTAL

Chemicals

Chitosan (Sigma Aldrich), glacial acetic acid (Fisher Scientific), triethyl orthoformate (Merck), RR, sodium hydroxide, sodium chloride and hydrochloric acid were purchased from Sinopharm Chemical Reagent Company Limited. All reagents were of analytical grade and were used as received. Distilled water was used in all preparations.

Synthesis of chitosan Schiff base

Firstly, 4-hydroxy-6-methyl-2,5-dioxo-5,6-dihydro-2H-pyrano[3,2-c]quinoline-3-carboxaldehyde was synthesized according to Othman *et al.* (2019). Chitosan (1 mol) was dissolved in 100 mL acetic acid 5% and stirred at 50 °C for 4 hours. The aldehyde (1 mol) was dissolved in the least amount of ethanol, then the solution was added dropwise to chitosan; the mixture was stirred at 70 °C for 24 hours. An orange gel of chitosan Schiff base was formed and collected by filtration, washed several times with a mixture of ethanol and acetone to remove any unreacted materials, and dried, giving a powder. The synthesis equation of chitosan Schiff base is illustrated in Figure 1(a).

Preparation of dye solution

A stock solution of 10^{-2} M of RR was prepared by dissolving the appropriate amount of dye in 25 mL of distilled water. The concentration needed for various steps of the investigation was prepared by dilution.

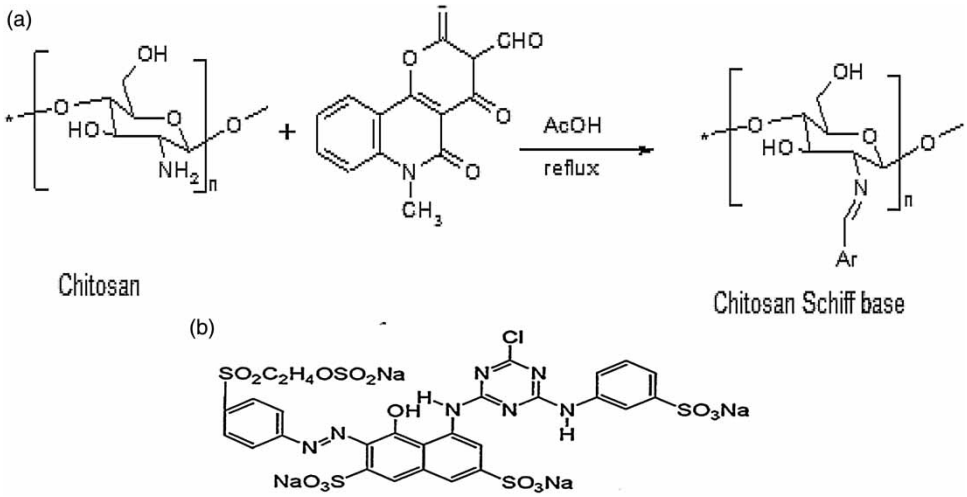

Figure 1 | Synthesis of chitosan Schiff base (a) and structure of remazol red dye (b).

Determination of pH_{zpc}

The pH point of zero charge (pH_{zpc}) of the adsorbent chitosan Schiff base was determined by the powder addition method (Ponnusami *et al.* 2008): 0.03 g of chitosan Schiff base was added to a 100 mL conical flask containing 10 mL of 0.1 M NaCl solution. Five samples were used for different initial pH solution, called pH_i. 0.1 M HCl and 0.1 M NaOH solution were used to reach the required pH values. After 24 hours the final pH (pH_f) was determined by pH meter Mettler Toledo.

Physicochemical characterization of chitosan Schiff base

FT-IR analysis

FT-IR measurements were performed using an FT-IR (Thermo Electron Corporation Nicolet avatar 370 CSL) with the wavenumber range 500–4,000 cm^{-1}.

XRD

X-ray diffractograms of chitosan and chitosan Schiff base samples were obtained using ARL™ X'TRA powder diffractometer (Thermo Fisher Scientific Inc.) with Cu-K-alpha wave length = 1.5405981 Å and current 44 mA – voltage 45 kV.

SEM

The chitosan Schiff base sample was analyzed using an SEM model Quanta 250 field emission gun (FEG) attached to an energy dispersive X-ray (EDX) analysis unit with accelerating voltage 30 kV, magnification 14x up to 1,000,000 and resolution for Gun.1n).

TGA

The sample was processed by Q500TA instruments.

Batch adsorption experiments

The equilibrium isotherm for adsorption was determined by using 0.1 g of adsorbent per 100 mL of aqueous solution for initial dye concentrations in the range of 10–100 ppm and pH = 5. For these experiments, the beakers were stirred at constant temperature (20 °C), for the contact time required to attain equilibrium. The solution samples were centrifuged after finishing the adsorption experiments at 7,000 rpm for 15 min. The effectiveness of the treatment was evaluated by measuring concentration by the UV-Visible spectroscopic method at $\lambda_{max} = 520$ nm. The same procedures were carried out to study the effect of pH by using different initial pH ranging from 3 to 11 and analyzing the residual color at the equilibrium contact time. The pH values were obtained using 0.1 M HCl and 0.1 M NaOH.

q_e(mg/g) is the amount of adsorption at equilibrium time t, and is calculated by:

$$q_e = (C_0 - C_e) \times V/W \quad (1)$$

where C_0 and C_e (mg/L) are the concentrations of dye at t = 0 min and at equilibrium time, respectively; V is the volume of dye solution (L); W is the mass of dry adsorbent used.

The kinetics were studied by stirring 0.1 gm of chitosan Schiff base into 100 mL of RR dye solution at different concentrations (10, 25, 50, 75, 100 ppm), and measured at different times, from 0 to 60 min. The adsorption process was carried out at 293 K (20 °C) and pH = 5 for all concentrations, except for the concentration of 50 ppm, which was also was performed at 293, 303, and 313 K. The aqueous samples were taken at contact time intervals, and the concentrations of dyes were similarly measured. The adsorption amount at time t, q_t (mg/g), was calculated using the following equation:

$$q_t = (C_0 - C_t)V/W \quad (2)$$

The percentage dye removal (R%) was calculated using Equation (3):

$$R\% = \frac{C_o - C_t}{C_o} \times 100 \quad (3)$$

RESULTS AND DISCUSSION

Characterization of the prepared chitosan Schiff base

FT-IR spectra

The FT-IR spectra of pure chitosan and chitosan Schiff base are illustrated in Figure 2. The spectra of pure chitosan showed the characteristic absorption peak of OH and NH_2 at 3,431 cm^{-1}. The peaks at 2,948 and 2,866 cm^{-1} are attributed to C–H stretching vibration. The characteristic absorption peaks of NH, $-CH_3$ and the second hydroxyl absorption peak (OH) appear at 1,619, 1,466 and 1,382 cm^{-1} respectively. For FT-IR spectra of chitosan Schiff base, there are two peaks at 1,748 (C = O α-pyrone), and 1,678 (C = O quinolone), in addition to the broad peak at around 3,424 cm^{-1} corresponding to the stretching vibration of N–H and O–H bonds shifted to a higher frequency (Xiaoxiao *et al.* 2009). Absorption bands at 1,531 cm^{-1} correspond to the N-H bending in secondary amides (amide II band), and those at 1,457.81, 889 cm^{-1} indicate OH in-plane bending, symmetrical C-H bending in CH_3 at 1,161 cm^{-1}. A peak at 1,015 cm^{-1} corresponds to C-O-C linkage, and 1,221 cm^{-1} corresponding to C-O stretching and 759 cm^{-1} corresponding to C-H bending can also be seen (Sashikala & Syed Shafi. 2014). A new absorption peak appeared at 1,634 cm^{-1}, which is assigned to the azomethine group vibration (C = N). These results indicate that chitosan Schiff base formed C = N groups at the N-position (Xiaoxiao *et al.* 2009).

XRD

Figure 3 shows the XRD patterns of the chitosan and chitosan Schiff base samples. The chitosan sample shows a strong peak at $2\Theta = 20.4°$. This suggests the formation of inter- and intra-molecular hydrogen bonds in the presence of free amino groups in chitosan. For the chitosan Schiff

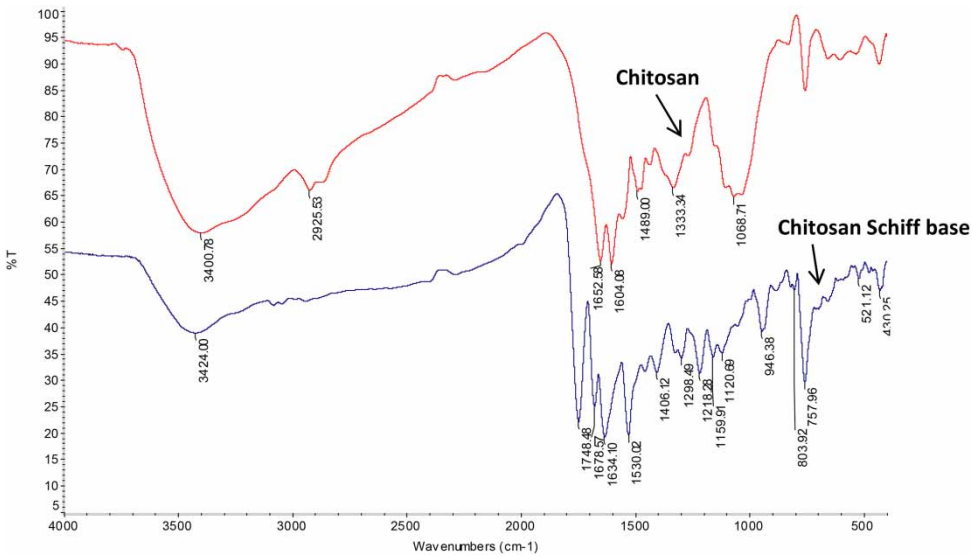

Figure 2 | FT-IR spectra of pure chitosan and of chitosan Schiff base.

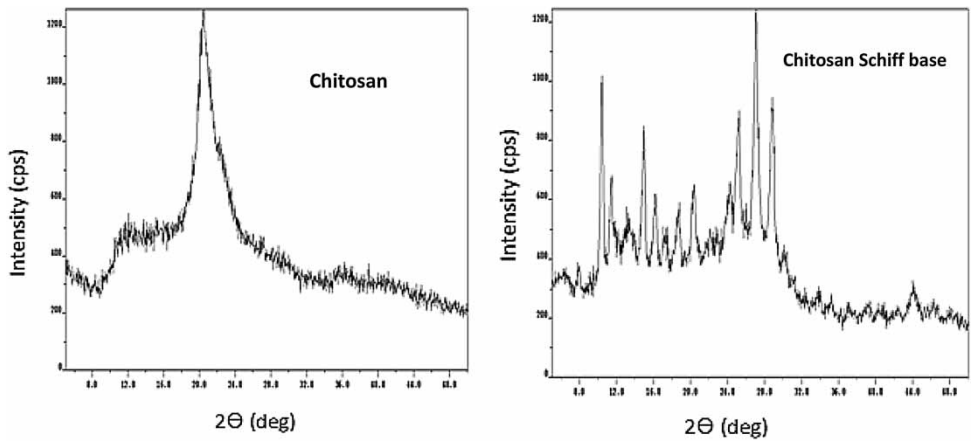

Figure 3 | X-ray diffraction patterns of chitosan and chitosan Schiff base.

base, the peak at 2Θ of 20.4° became broader and less intense; this reflects a more amorphous nature. This is probably due to the deformation of the strong hydrogen bond in the chitosan backbone with the substitution of quinolinone aldehyde on the N-atom of chitosan (Salama *et al.* 2015; Xiaoxiao *et al.* 2016). In addition, there was higher semi-crystalline nature of the blend, which was identified by the broad amorphous peak indicating that there was a molecular miscibility and an interaction between chitosan and the pyranoquinolinone moiety (Sashikala & Syed Shafi 2014).

TGA

The thermal stability was assessed by TGA analysis, as shown in Figure 4. TGA is a good technique to determine the thermal stability of polymers and their blends. It is important for measuring the mass of the substance as a function of temperature, while the substance is exposed to a controlled temperature programme (Sashikala & Syed Shafi 2014). From the TGA curves, chitosan weight loss was observed at 281 °C which corresponds to chitosan moieties. For chitosan Schiff base, weight loss was observed at 343.05 °C. The temperature difference observed might be due to formation of chitosan Schiff. Our result proves the higher stability of chitosan Schiff base at higher temperatures.

SEM

Figure 5 shows SEM images of chitosan Schiff base; they reveal a significant surface roughness of the new composite material. This is attributed to the loss of hydrogen bonds in the chitosan chains due to chitosan Schiff base

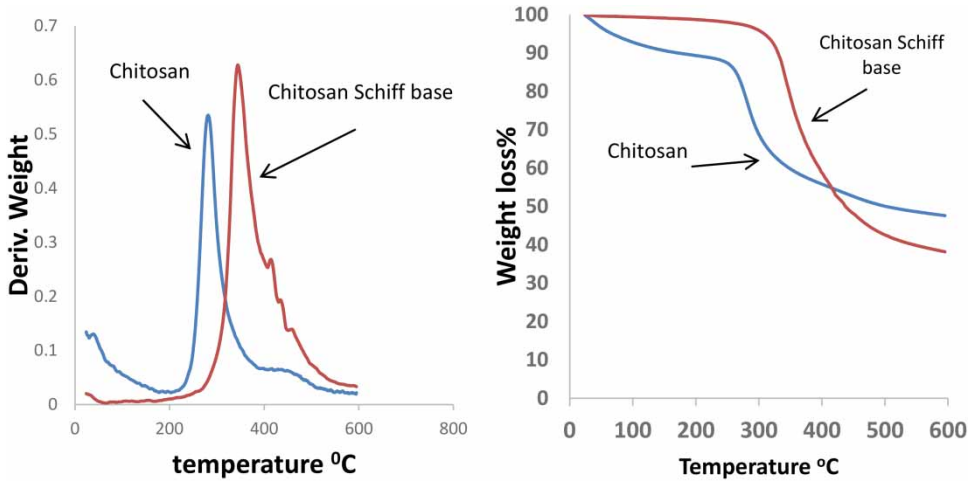

Figure 4 | The thermal stability of pure chitosan and that of the chitosan Schiff base.

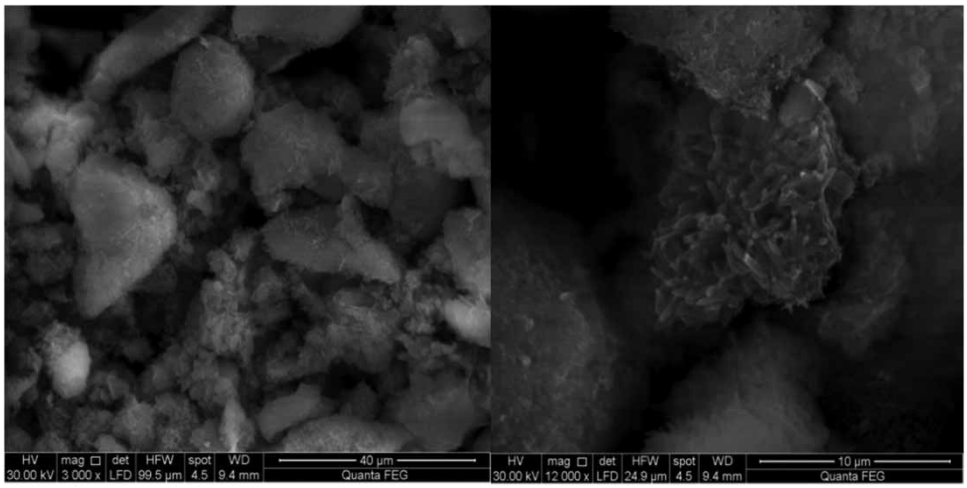

Figure 5 | SEM image of solid chitosan Schiff base.

formation (Huanhuan *et al.* 2018). The incorporation of the bulky pyranoquinolinone group into chitosan polymer matrices also creates surface roughness (Amtul *et al.* 2018). The SEM image of the powdered chitosan Schiff base indicates a polymorphic porous structure (Santosh *et al.* 2014).

Adsorption experiments

Effect of dye concentration

By studying the effect of RR dye concentration ranging from 10 to 100 ppm on the removal of RR, we found that the R% of dye removal by chitosan Schiff base increased with increasing initial dye concentration, as shown in Figure 6, from 10 to 50 ppm, which can be explained in the terms of the presence of unsaturated sites in the chitosan Schiff base morphology. Only 50 ppm dye concentration was needed to achieve 100% dye removal. But when the concentrations of dye were higher (>50 ppm) the rate of adsorption decreased and the Figure 6 curve did not show the same asymptotic form. This may be due to all vacant sites in the chitosan Schiff base morphology being saturated by the dye molecules (El-Harby *et al.* 2017).

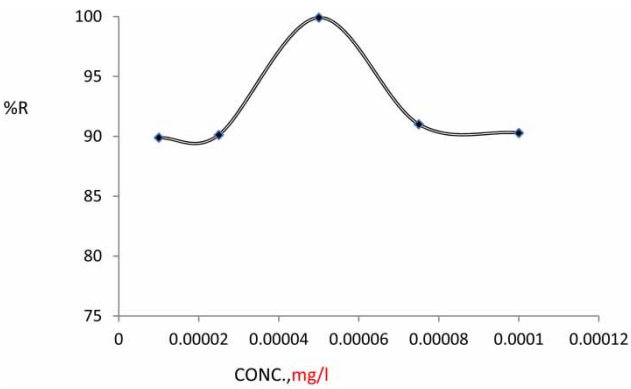

Figure 6 | Effect of RR dye concentration on the adsorption process at equilibrium time [pH = 6, 293 K, adsorbent dose = 0.1 g].

pH of dye solution

The effect of pH on the adsorption of RR dye onto chitosan Schiff base at equilibrium time [dye concentration = 50 ppm, temperature = 293 K, chitosan Schiff base dose = 0.1 g] is shown in Figure 7(a) and 7(b). Removal of RR dye increased at low pH (≤7). It is known that the pH_{pzc} value affects a net zero charge on a solid surface in the absence of specific sorption (Elbadawy 2016). The pH_{pzc} of chitosan Schiff base was determined by the powder addition method (Elbadawy 2016), as recorded in experimental section. Both positive and negative $-\Delta pH$ ($pH_i - pH_f$) values were recorded for the chitosan Schiff base and plotted against the initial pH_i values, as shown in Figure 7(b). The zero point charge of chitosan Schiff base was found to be 5.9. So, anion adsorption onto chitosan Schiff base will be favorable at $pH \leq pH_{zpc}$, where the surface of the adsorbent becomes positively charged and favors the uptake of anionic dyes due to the increasing electrostatic force of attraction. Thus, RR adsorption onto chitosan Schiff base is increased at lower pH (<5.9). The opposite happened at high pH ($>pH_{zpc}$); the adsorbent surface was negatively charged, so, it repelled the negatively charged RR anions from vacant adsorption sites, causing

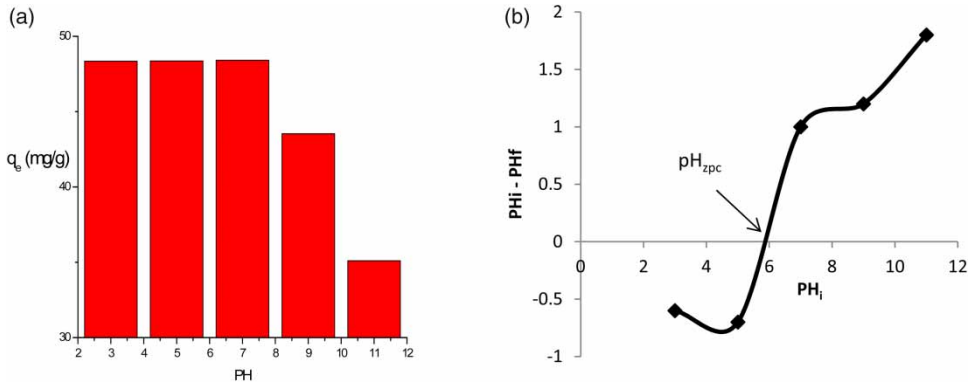

Figure 7 | (a) Effect of pH of RR dye solution on adsorption capacity of chitosan Schiff base at equilibrium time [dye concentration = 50 ppm, 293 K, chitosan Schiff base dose = 0.1 g] and (b) ΔpH versus pH_i.

a decrease in dye sorption (q_e values). Also, in a previous study, Jiang *et al.* (2013) reported that in acidic solutions chitosan is easily protonated to form positive groups because of the presence of amino groups. So, the surface of chitosan at low pH values will be positively charged but increasing pH values will gradually cause the surface to become negative at high pH (the isoelectric point of chitosan Schiff base is at pH = 5.9). However, the equilibrium time of adsorption process decreased by decreasing the pH of dye solution; at pH = 3 the adsorption removal percentage of chitosan Schiff base reached 100% in only 2 min. The results obtained indicate that ion diffusion act as physical forces effects on the behavior of dye molecules (the adsorbates) in the proximity area of the adsorbent, chitosan Schiff base. The same behavior was observed for the adsorption of remazol brilliant violet onto chitosan 10b flakes (Wan Ngaha *et al.* 2011).

Dosage and contact time influence on chitosan Schiff base

The effects of dosage and contact time on the removal of RR by chitosan Schiff base by varying the dosage from 0.03 to 0.15 g, keeping all other parameters constant, as shown in Figure 8. This figure shows that the amount of dye removed from the aqueous solution increased with increasing dosage of chitosan Schiff base from 0.03 to 0.1 g. But further increasing the adsorbent dose to 0.15 g did not change the R%. However, 0.1 g adsorbent dosage was sufficient to achieve 100% removal of dye from a 50 ppm dye solution and a further increase in the dosage was not required. It is obvious that an increase in adsorbent dosage increases available surface area and active sites. So, 0.1 g of chitosan Schiff base adsorbent was sufficient in all the RR adsorption experiments.

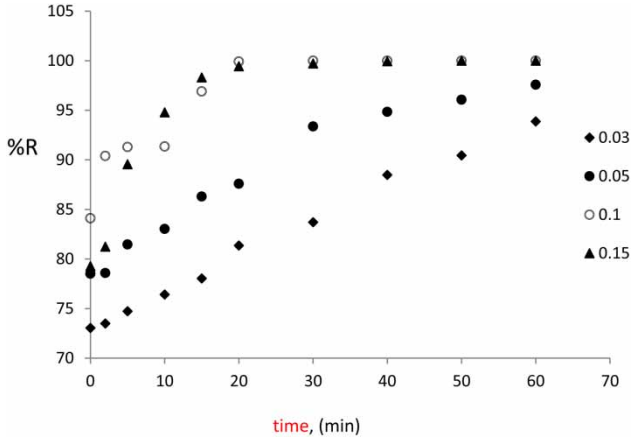

Figure 8 | Influence of dosage of chitosan Schiff base on R% of RR dye [dye concentration = 50 ppm, 293 K, pH = 6].

In studying the effect of contact time in Figure 8, it is clear that by using a chitosan Schiff base dose ≥0.1 g, equilibrium was attained within a short time interval (a plateau was reached in 20 min). Dye removal was rapid in the initial stage (R% = 100%) and stayed constant with the increase of time. This initial increase was due to the presence of a large number of vacant sites and with the passage of time, the number of active sites decreased, hence the reduction in the adsorption rate. Conversely, the equilibrium time increased with a decrease in the dose of chitosan Schiff base < 0.1 g, which reached 60 min (R% = 100%). This result highlights the high efficiency of the prepared modified polymer for RR dye removal compared with a previous study carried out on the adsorption of Congo red dye onto terephthaloyl thiourea cross-linked chitosan, where the adsorption equilibrium time was not reached until 200 min (El-Harby *et al.* 2017).

Finally, we can say that the synthesized chitosan Schiff base was shown to be a hopeful adsorbent for the removal

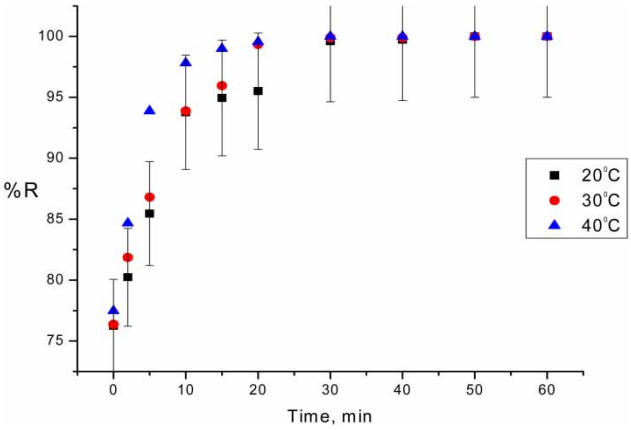

Figure 9 | Effect of temperature of RR dye solution on its R% by chitosan Schiff base at different times [dye concentration = 50 ppm, pH = 6, chitosan Schiff base dose = 0.1 g].

of the textile dye RR from aqueous solutions. This is further emphasized by comparison with the maximum adsorption capacity of textile dye with different adsorbents with q_{max} of chitosan solids, as will be mentioned in the next isotherm study part.

Effect of temperature

The influence of temperature on the percentage dye removal onto chitosan Schiff base was studied at different temperatures: 20, 30, and 40 °C, as shown in Figure 9. It is clear that increasing the dye solution temperature increases the amount of adsorption, which confirms a kinetically controlled endothermic adsorption process. Therefore, higher temperatures facilitate the adsorption of RR onto chitosan Schiff base, because the mobility of dye molecules and their diffusion increased with increasing temperature (Wan Ngaha *et al.* 2011; Badawy *et al.* 2019). The higher removal due to increasing temperature may be attributed to chemical interactions taking place between the functional groups of the adsorbent and the dye. Also, Figure 9 shows that the shortest adsorption equilibrium time for RR dye adsorption by chitosan Schiff base was obtained at 40 °C. This may be attributed to the tumefaction effect that increasing temperature may have produced within the inner structure of chitosan Schiff base, which facilitated the penetration of dye molecules into its internal structure.

Kinetic studies and mechanism of adsorption process

Kinetic studies are commonly applied to understand the mechanism of adsorption reactions. In our study we used the pseudo-first-order, pseudo-second-order, intra-particle diffusion and Elovich models and their equations (El-Harby *et al.* 2017; Tran *et al.* 2017; Elham *et al.* 2019).

Normalized standard deviation, S.D. (%), is also applied to find the most applicable model to describe the kinetic study of adsorption of RR dye on the investigated adsorbent. S.D. (%) was calculated using Equation (4)

$$\text{S.D. (\%)} = 100 \times \frac{\sqrt{[qt(exp) - qt(cal)/qt(exp)]2}}{N - 1} \quad (4)$$

where the number of data points is N, and the experimental and calculated values of adsorption capacity are $q_{t(exp)}$ and $q_{t(cal)}$, respectively.

Based on the values of S.D. (%) and R^2 given in Table 1, it is clear that the pseudo-second-order model is the best for describing the adsorption kinetics of RR dye onto chitosan Schiff base at different temperatures.

By applying the pseudo-first-order and pseudo-second-order models for adsorption of RR onto chitosan Schiff base sample at concentrations in the range 10–100 ppm at 20 °C as shown in Figure 10(a) and 10(b), we found that pseudo-second-order model was the best fit for our experimental data. The values of $q_{e(exp)}$, K_1, K_2, $q_{e(cal)}$, the corresponding linear regression coefficient R^2 values and calculated S.D. (%) are summarized in Table 1 (K_1 (min^{-1}) is the pseudo-first order constant, K_2 (g/mg·min) is the pseudo-second-order constant). We can summarise the results obtained from this table as follows: (i) R^2 and S.D. (%) and the value of the pseudo-second-order model were up to 0.998 and <0.683, respectively, but R^2 and S.D. (%) and the values of the pseudo-first-order model ranged between 0.03–0.93 and 31.42–29.06, respectively. (ii) At 20 °C, K_2 values for dye concentration ≤50 ppm were higher than that at 75 and 100 ppm. (iii) $q_{e(exp)}$ was a better fit with $q_{e(cal)}$ (pseudo-second-order) than $q_{e(cal)}$ (pseudo-first-order), which confirmed that the adsorption process was pseudo-second-order. The above results emphasize the matching of pseudo-second-order model with our experimental data and that it was appropriate for the adsorption process.

The intra-particle diffusion model was plotted in Figure 10(c); the values of the intra-particle diffusion rate constants, K_{dif1}, K_{dif2} and R^2 are given in Table 1. The good linearity of the plots indicates that intra-particle diffusion may play an important role in the first stage of adsorption. As the initial concentration of the dye increases, the intra-particle diffusion rate constant (K_{dif}) increases

Table 1 | Kinetic parameters models for RR adsorption onto chitosan Schiff base

		Pseudo-first-order				Pseudo-second-order					Intra-particle diffusion step 1	Intra-particle diffusion step 2	Elovich's kinetic model
Temp.	Conc.	K_1 min^{-1}	$q_{e(cal)}$ (mg/g)	R^2	S.D. (%)	$q_{e(exp)}$ (mg/g)	K_2 (g/mg min)	$q_{e(cal)}$ (mg/g)	R^2	S.D. (%)	$K_{Dif\ 1}$ (mg/gmin$^{-0.5}$)	K_{Dif2} (mg/gmin$^{-1/2}$)	β (g mg^{-1}) α (g mg^{-1} min^{-1})
20 °C	10 ppm	0.0159	1.0386	0.0307	29.37	8.74	0.360	8.802	0.999	0.236	2.4 $R^2 = 0.937$	0.068 $R^2 = 0.963$	β 2.271 α 5.5×10^6 R^2 0.845
	25 ppm	0.108	2.756	0.886	29.49	23.91	0.0507	23.42	0.998	0.683	0.79 $R^2 = 0.932$	0.670 $R^2 = 0.971$	β 0.61255 α 0.06×10^6 R^2 0.845
	50 ppm	0.203	2.765	0.932	31.42	48.41	0.0506	48.78	0.999	0.255	1.92 $R^2 = 0.9479$	0.734 $R^2 = 0.871$	β 0.5883 α 9.1×10^{10} R^2 0.8312
	75 ppm	0.564	6.613	0.638	30.28	72.28	0.0168	71.42	0.998	0.396	1.96 $R^2 = 0.9674$	1.829 $R^2 = 0.9854$	β 0.21514 α 0.37×10^6 R^2 0.962
	100 ppm	0.953	12.304	0.634	29.06	95.99	0.00143	95.24	0.998	0.260	3.052 $R^2 = 0.9784$	1.485 $R^2 = 0.963$	β 0.1746 α 1.9×10^6 R^2 0.967
30 °C	50 ppm	0.151	2.795	0.935	29.37	48.41	0.0424	48.78	0.999	0.236	–	–	–
40 °C	50 ppm	0.058	1.755	0.379	29.49	48.41	0.084	48.78	0.999	0.683	–	–	–

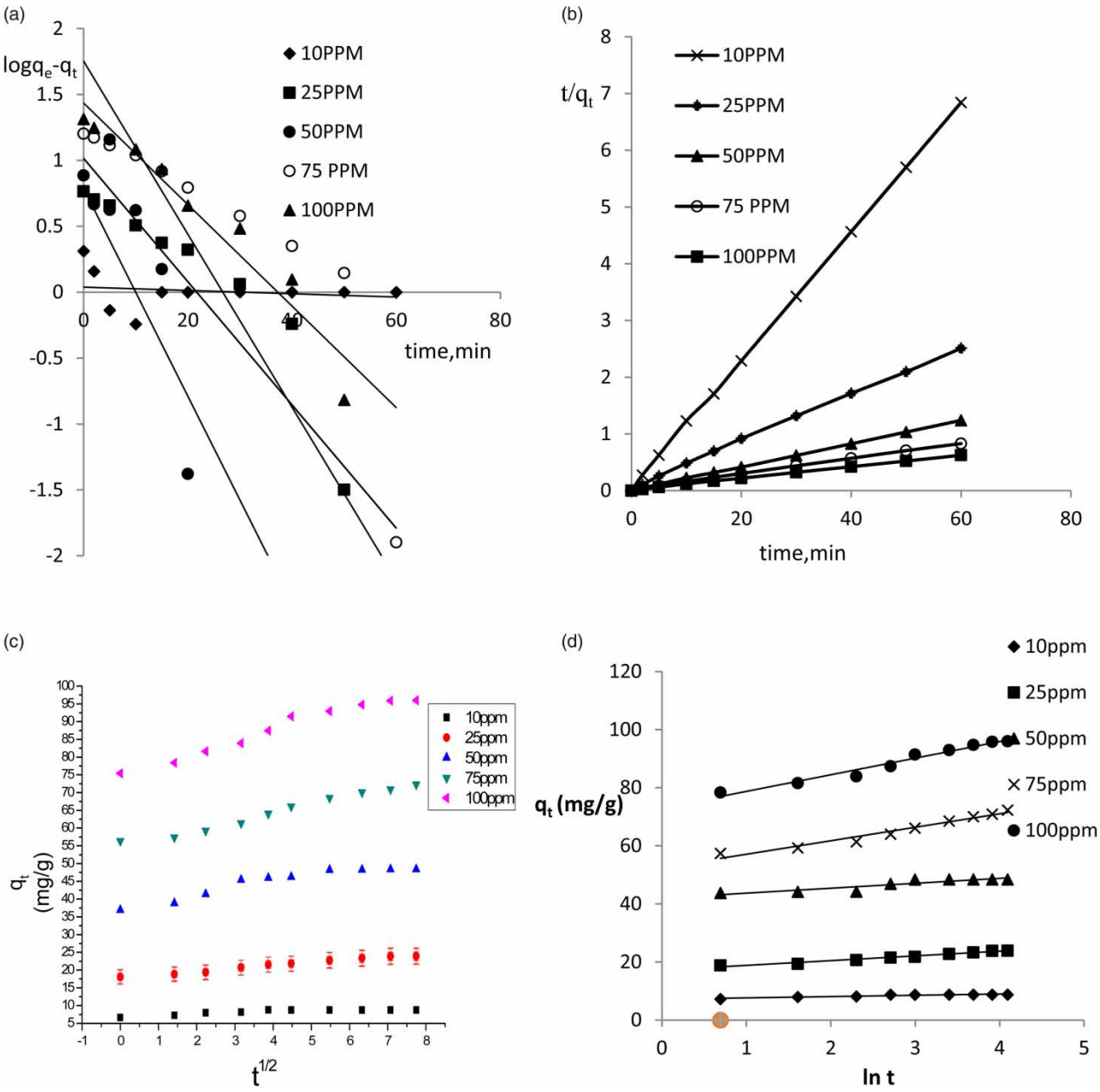

Figure 10 | (a) Pseudo-first-order, (b) pseudo-second-order, (c) intra-particle diffusion, and (d) Elovich's kinetic models for RR adsorption onto chitosan Schiff base at 20 °C.

(Table 1). This may be related to intra-particle diffusivity as well as K_{dif} being directly related to q_e.

It is known that when the plot q_t versus $t_{0.5}$ passes through the origin, the intra-particle diffusion becomes the sole rate-limiting step. But in our study the intra-particle transport is not the rate-limiting step due to the deviation of the straight lines from the origin and so the mechanism comprises simultaneous adsorption and intra-particle diffusion (Figure 10(c)) (El-Harby *et al.* 2017; Murcia-Salvador *et al.* 2019). The results obtained indicate that the molecules of RR dye adsorbed quickly onto the sorbent surface at the beginning of the adsorption process, and then intra-particle diffusion slowed down and stabilized.

Figure 10(d) refers to Elovich's kinetic model, which is for chemical adsorption processes. The Elovich constants can be calculated from the slope and intercept of the line obtained by plotting q_t vs. ln t (Figure 10(d)) and listed in Table 1. The results obtained show that the R^2 values of

this kinetic model were rather low; this model was not applicable to RR adsorption by chitosan Schiff base. This means that the adsorption system is closer to physical adsorption (Elham *et al.* 2019).

It is clear from previous results that the modification of chitosan led to new active basic sites for adsorption besides the decreasing the crystalline size of chitosan Schiff base, as obtained in XRD results. This likely increases the chemical interaction of RR dye with our adsorbent. Secondly, the relation between the RR structure and the surface charge of chitosan Schiff base must be borne in mind. Studying the effect of pH showed that the dye solution at a pH below the zero point charge ($pH_{pzc} = 5.9$) of the adsorbent made the surface of the sorbent positively charged and able to attract the negatively charged dye from the solution. So, an electrostatic attraction exists between the positively charge surface of the adsorbent and the negative charge of the RR dye (due to the presence of three SO_3 groups on each molecule, Figure 1(b)). On the other hand, further poor adsorption was observed in the basic pH range ($pH > 7$). It may have been due to the deprotonation of functional groups giving rise to electrostatic repulsion with RR dye. The results showed that the modification of chitosan with pyranoquinolinone could improve the adsorbent's efficiency, relying on the chemical adsorption conditions (pH and dye concentration), the properties of the particles (PZC) and the control of adsorbent dose.

Isotherm study

Batch experiments were performed at different dye concentrations varying from 10 to 100 ppm. Samples were taken and analyzed several times until equilibrium was attained. By applying Freundlich, Langmuir, Temkin and Dubinin–Radushkevich equations (El-Harby *et al.* 2017; Tran *et al.* 2017; Ahmed *et al.* 2019; Fatima-Zahra *et al.* 2019), the data of Freundlich isotherm were obtained by the plot of log q_e versus log C_e as in Figure 11, where q_e is the amount of dye adsorbed at equilibrium time (mg/g), and C_e is equilibrium concentration dye in solution (mg/L). Different Freundlich isotherm parameters K_F and 1/n were determined by linear regression, and R^2 values are listed in Table 2. K_F is the Freundlich constant (L/mg) related to the bonding energy and 1/n is the heterogeneity factor. The values of 1/n and K_F were 0.945 and 1.96 L/mg, respectively. It is known that the adsorption process is favorable when the value of 1/n is lower than 1 and this was confirmed for chitosan Schiff base (El-Harby *et al.* 2017). Also, we found that the obtained data fit well with the Freundlich isotherm, yielding a high R^2 value (0.982), close to 1.0.

The straight line of the Langmuir isotherm was obtained by plotting C_e/q_e versus C_e (Figure 11), whose parameters q_{max} (maximum adsorption capacity), and K_L (Langmuir constant) were determined from its slope and the intercept, respectively. R^2 also was determined and listed in Table 2. The value of R^2 is lower than that obtained with the Freundlich isotherm. Previous studies have been carried out using chitosan polymer for the adsorption of different dyes and similar results were obtained (Subramani & Thinakaran 2017; Murcia-Salvador *et al.* 2019).

By applying the Langmuir equation, the q_m value obtained was 344 mg/g. A comparison of the maximum adsorption capacities of RR dye onto chitosan Schiff base in this work was done as shown in Table 3. The results show that the q_m of RR dye onto chitosan Schiff base is higher than q_m in other studies of anionic dyes with different modified chitosan adsorbents (Demarchi *et al.* 2015; Salama *et al.* 2015; Othman *et al.* 2019).

The Temkin isotherm explains the influences of indirect adsorbate/adsorbate interactions on adsorption isotherms (Fatima-Zahra *et al.* 2019). The values of α_t and b_t were determined from the intercept and the slope of the linear plots and given by plotting q_e versus $\ln C_e$ in Figure 11. The resulting parameters α_t, b_t and R^2 are listed in Table 2. The values of R^2 and b_t for chitosan Schiff base are 0.9705 and 86.4 kJ/mol, respectively. The positive value of b_t shows that there are physical as well as chemisorption processes in the adsorption process (Murcia-Salvador *et al.* 2019).

The Dubinin–Radushkevich (D–R) isotherm is compatible between Gaussian energy distribution and adsorption processes on a heterogeneous surface (Ahmed *et al.* 2019). The value of E is useful to predict the type of sorption reaction. If E is in the range of 8–16 kJ mol^{-1}, the sorption is governed by chemical ion exchange. In the case of $E < 8$ kJ mol^{-1}, physical forces may affect the sorption. From the results of the D–R model shown in Figure 11 and Table 2, we found that the E magnitude was 500 J mol^{-1}, which indicating that the sorption was governed by physical adsorption (Ahmed *et al.* 2019).

Adsorption thermodynamics

Thermodynamic parameters such as the standard free energy change (ΔG°), standard enthalpy change (ΔH°), and standard entropy change (ΔS°) of RR adsorption on chitosan Schiff base were calculated at different temperatures: 20, 30

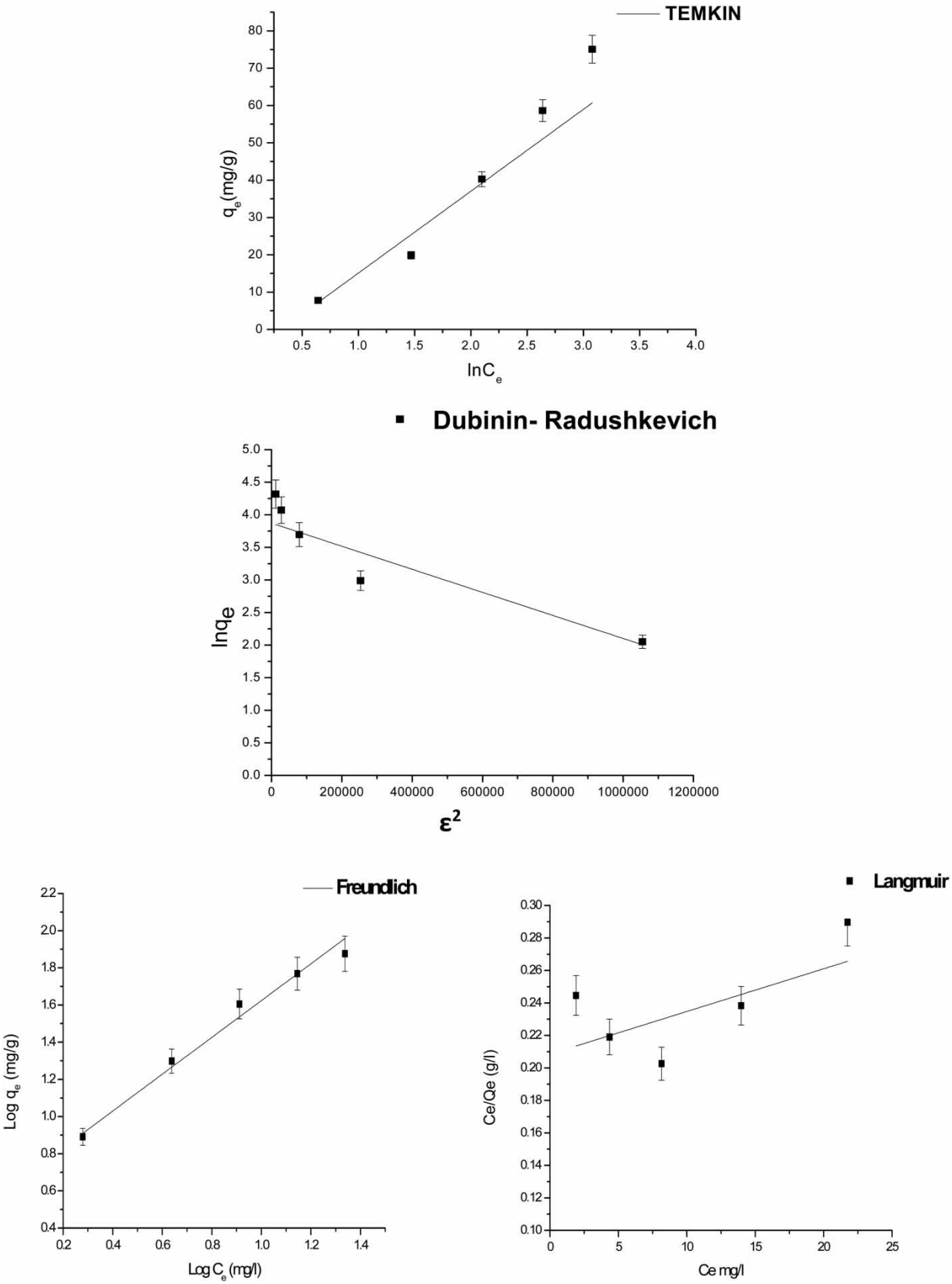

Figure 11 | Freundlich, Langmuir, Temkin, and Dubinin–Radushkevich isotherms for RR dye adsorption onto chitosan Schiff base.

Table 2 | Isotherm adsorption parameters (Langmuir, Freundlich, Dubinin–Radushkevich, and Temkin models), for adsorption of RR onto chitosan Schiff base

Isotherm	Parameters		Isotherm	Parameters	
Freundlich	1/n	0.945	Dubinin–Radushkevich	q_m (mg/g)	53.51
	R^2	0.982		E (J/mol)	500
	K_F (L/mg)	1.96		K	0.000002
				R^2	0.8812
Langmuir	q_m (mg/g)	344.8	Temkin	α_t	1.739
	K_L (L/mg)	1.23		R^2	0.9705
	R^2	0.479		b_t	86.4

Table 3 | Comparison of adsorption capacity of different anionic dyes by modified linked chitosan adsorbents

No.	Chitosan adsorbent	Dye	Adsorption capacity (mg/g), q_m	Reference
1	Chitosan polyacrylamide composite hydrogels	Congo red	2.1×10^{-4} mol g^{-1}	Salama *et al.* (2015)
2	Terephthaloyl thiourea cross-linked chitosan hydrogels (TTU-chitosan-1)	Congo red	44.248	El-Harby *et al.* (2017)
3	Chitosan	Remazol red	155.72	Othman *et al.* (2019)
4	Chitosan-liked p-t-butylcalix[4]arene	Remazol yellow FG	188.31	Demarchi *et al.* (2015)
5	**Chitosan Schiff base**	**Remazol red**	**344.80**	**Present study**
6	GLA cross-linked chitosan	Reactive red	7.50	Cestari *et al.* (2004)
7	GLA cross-linked chitosan	Congo red	24.18	Feng *et al.* (2011)
8	Terephthaloyl thiourea cross-linked chitosan hydrogels (TTU-chitosan-3)	Congo red	37.70	El-Harby *et al.* (2017)
9	Terephthaloyl thiourea cross-linked chitosan (TTU-chitosan-2)	Congo red	38.70	El-Harby *et al.* (2017)

and 40 °C (293, 303, and 313 K). The values of ΔG°, ΔH° and ΔS° were calculated according to the Gibbs free energy equations:

$$\Delta G^\circ = -RT \ln K_C \quad (5)$$

$$\ln K_C = \Delta S^\circ/R - \Delta H^\circ/RT \quad (6)$$

where R is the universal gas constant (8.314 J/mol K), T is the absolute solution temperature (K), and K_C is the variation of the thermodynamic equilibrium constant. In this method, K_d values are obtained by plotting ln (q_e/C_e) against C_e (figure not given), then K_d is converted to K_C by multiplying K_d by a factor of 1,000 (Tran *et al.* 2017). ΔH° and ΔS° were obtained from the slope and intercept of van 't Hoff plots of $\ln K_C$ vs. 1/T (Figure 12) and the thermodynamic parameters are presented in Table 4. Table 4 shows that the positive value of the standard enthalpy of adsorption ΔH° for RR on chitosan Schiff base is obtained from the slope of the plot between ln K_C versus 1/T, indicating that the adsorption of RR by chitosan Schiff base is endothermic, which is supported by the increasing adsorption of RR with increasing temperature, while the negative values of ΔG° are evidence that

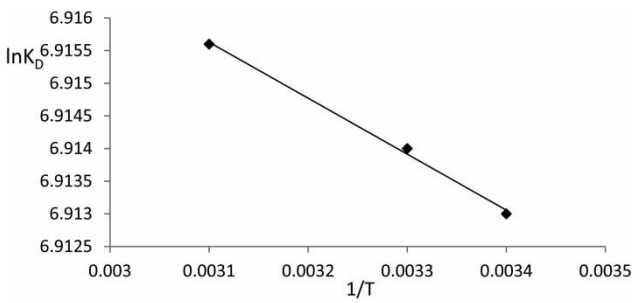

Figure 12 | The van 't Hoff plots $\ln K_D$ vs. 1/T for RR dye adsorption onto solid chitosan Schiff base.

Table 4 | Thermodynamic parameters for adsorption of RR on to chitosan Schiff base

Temperature (K)	ΔH (kJ mol^{-1})	ΔS (kJ mol^{-1} K^{-1})	ΔG (kJ mol^{-1})
293	71.13	57.72	−16.81
303			−17.38
313			−17.96

the adsorption reaction is a spontaneous process and more favorable at high temperature. On the other hand, the positive value of ΔS° showed the increasing of randomness at the solid/solution interface during the sorption process.

CONCLUSION

The novel adsorbent of modified chitosan bearing pyranoquinolinone moiety was successfully synthesized. In our study, this adsorbent showed the greatest ability to adsorb a textile carcinogenic organic dye from aqueous solution. The maximum adsorption capacity was 344.4 mg/g. Several factors affected the adsorption capacity of this synthesized sample: temperature, pH, initial concentration of the dye solution, dose of adsorbent and contact time with the RR dye. The results obtained showed that chitosan Schiff base achieved a dye uptake percentage of 100% after a period of dye contact time not exceeding 2 min. Pseudo-first-order, pseudo-second-order, intra-particle diffusion, and Elovich adsorption kinetic models along with Langmuir, Freundlich, Temkin, and Dubinin–Radushkevich adsorption isotherms models were utilized in this study. The sorption process was better fitted to pseudo-second-order equation and the Freundlich model. The mechanism of dye removal from its aqueous solution over chitosan modified with pyranoquinolinone was proposed. In addition, thermodynamic parameters for dye adsorption were calculated.

FUNDING

This research did not receive any specific grant from funding agencies in the public, commercial, or not-for-profit sectors.

REFERENCES

Ahmed, R., Inas, A. & Dina, B. 2019 The removal of brilliant green dye from aqueous solution using nano hydroxyapatite/chitosan composite as a sorbent. *Molecules* **24**, 847.

Amtul, J. S., Yasha, N. B. & Sitara, N. 2018 Elimination of a carcinogenic anionic dye Congo red from water using hydrogels based on chitosan, acrylamide and graphene oxide. *Journal of Bioprocessing & Biotechniques* **8**, 2155–9821.

Badawy, A. A., Ibrahim, S. M. & Hisham, A. E. 2019 Enhancing the textile dye removal from aqueous solution using cobalt ferrite nanoparticles prepared in presence of fulvic acid. *Journal of Inorganic and Organometallic Polymers and Materials* **30**, 1798–1813. https://doi.org/10.1007/s10904-019-01355-1.

Blackburn, R. S. 2004 Natural polysaccharides and their interactions with dye molecules: applications in effluent treatment. *Environmental Science & Technology* **38**, 4905–4909.

Cestari, A. R., Vieira, E. F. S., dos Santos, A. G. P., Mota, J. A. & de Almeida, V. P. 2004 Adsorption of anionic dyes on chitosan beads: the influence of the chemical structures of dyes and temperature on the adsorption kinetics. *Journal of Colloid and Interface Science* **280**, 380–386.

Demarchi, C. A., Debrassi, A., de Campos Buzzi, F., Nedelko, N., Ślawska-Waniewska, A., Dłużewski, P., Dal Magro, J., Scapinello, J. & Rodrigues, C. A. 2015 Adsorption of the dye Remazol Red 198 (RR198) by O-carboxymethylchitosan-N-lauryl/c-Fe_2O_3 magnetic nanoparticles. *Arabian Journal of Chemistry* **12** (8), 3444–3453. http://dx.doi.org/10.1016/j.arabjc.2015.08.028.

Elbadawy, A. K. 2016 N-succinyl chitosan–dialdehyde starch hybrid hydrogels for biomedical applications. *Journal of Advanced Research* **7**, 69–77.

Elham, B. A., Alireza, B. & Jahan, B. G. 2019 Efficient removal of malachite green from wastewater by using boron-doped mesoporous carbon nitride. *Applied Surface Science* **469**, 236–245.

El-Harby, N. F., Ibrahim, S. M. A. & Mohamed, N. A. 2017 Adsorption of Congo red dye onto antimicrobial terephthaloyl thiourea cross-linked chitosan hydrogels. *Water Science & Technology* **76**, 2719–2732.

Fatima-Zahra, B., Tarik, A. & Fouzia, B. 2019 Kinetic study of adsorption methylene blue dye from aqueous solutions using activated carbon from starch. *Chemical Review and Letters* **2**, 33–39.

Feng, T., Zhang, F., Wang, J. & Huang, Z. 2011 Adsorption of Congo red by cross-linked chitosan film. In: *Bio-informatics and Biomedical Engineering (iCBBE)*. IEEE, China, pp. 1–4.

Geyse, A. C. R., Domingos, S. A. S., Clayane, C. S., Adriana, P. V., Cícero, W. B. B., Auro, A. T. & Sirlane, A. A. S. 2017 Removal of Remazol brilliant violet textile dye by adsorption using rice hulls. *Polímeros* **27**, 16–26.

Huanhuan, M., Aiqun, K., Yanhong, J., Benqiao, H., Yunfei, S. & Jianxin, L. 2018 Ultrahigh adsorption capacities for anionic and cationic dyes from wastewater using only chitosan. *Journal of Cleaner Production* **214**, 89–94. https://doi.org/10.1016/j.jclepro.2018.12.217.

Jiang, H., Chen, P., Luo, Sh., Tu, X., Cao, Q. & Shu, M. 2013 Synthesis of novel nanocomposite Fe_3O_4/ZrO_2/chitosan and its application for removal of nitrate and phosphate. *Applied Surface Science* **284**, 942–949.

Manchaiah, A. S. & Badalamoole, V. 2019 Novel heterocyclic chitosan-based Schiff base: evaluation as adsorbent for removal of methyl orange from aqueous solution. *Water and Environment Journal* **0**, 1–10.

Manimohan, M., Pugal Mani, S. & Mohamed, A. S. 2019 Zinc(II) centered biologically active novel N,N,O donor tridentate water-soluble hydrazide-based O-carboxymethyl chitosan

Schiff base metal complexes: synthesis and characterization. *New Journal of Chemistry* **43**, 9540–9554.

Murcia-Salvador, A., José, A., Pellicer, M., Fortea, I., Vicente, M. G., María, I. R., Núñez-Delicado, E. & Gabaldón, J. A. 2019 Adsorption of direct blue 78 using chitosan and cyclodextrins as adsorbents. *Polymers* **11**, 1003.

Nuriye, K., Mustafa, S., Semahat, K. & Zehra, O. E. 2012 Synthesis and characterization of novel nano-chitosan Schiff base and use of lead (II) sensor. *International Journal of Biological Macromolecules* **51**, 1159–1166.

Othman, E. S., Hassanin, H. M. & Mostafa, M. A. 2019 Synthesis of Pyrano[3,2-c]quinoline-3-carboxaldehyde and 3-(Ethoxymethylene) –pyrano [3,2-c] quinolinone and their chemical behavior toward some nitrogen and carbon nucleophiles. *Journal of Heterocyclic Chemistry* **56**, 1598.

Ponnusami, V., Vikram, S. & Srivastava, S. N. 2008 Guava (*Psidium guajava*) leaf powder: novel adsorbent for removal of methylene blue from aqueous solutions. *Journal of Hazardous Materials* **152**, 276–286.

Salama, H. E., Saad, G. R. & Sabaa, M. W. 2015 Synthesis, characterization and biological activity of Schiff bases based on chitosan and arylpyrazole moiety. *International Journal of Biological Macromolecules* **79**, 996–1003.

Santosh, K., Mridula, K., Dutta, P. K. & Joonseok, K. 2014 Chitosan biopolymer Schiff base: preparation, characterization, optical and antibacterial activity. *International Journal of Polymeric Materials and Polymeric Biomaterials* **63** (4), 173–177.

Sashikala, S. & Syed Shafi, S. 2014 Synthesis and characterization of chitosan Schiff base derivatives. *Scholars Research Library* **6**, 90–97.

Saud, A. A., Jawada, A. H. & AbdulKarim-Talaq, M. 2019 Synthesis of chitosan-ethylene glycol diglycidyl ether/TiO_2 nanoparticles for adsorption of reactive orange 16 dye using a response surface methodology approach. *Bioresource Technology* **293**, 122071.

Subramani, S. & Thinakaran, N. 2017 Isotherm, kinetic and thermodynamic studies on the adsorption behaviour of textile dyes onto chitosan. *Process Safety and Environmental Protection* **106**, 1–10.

Swathi, B., Ravi, K. M., Satyanarayana, B., Pandu, N. C., Ramesh, Y., Sruthi, V., Rajendra, K. J., Raghu, B. K. & Paul, D. S. 2016 Magnetic nano cobalt ferrite catalyzed synthesis of 4H-Pyrano[3,2-h]quinoline derivatives under microwave irradiation. *Green and Sustainable Chemistry* **6**, 101–109.

Tanhaei, B., Ayati, A., Bamoharram, F. F., Lahtinenc, M. & Sillanpaa, M. 2016 A novel magnetic Preyssler acid grafted chitosan nano adsorbent: synthesis, characterization and adsorption activity. *Journal of Chemical Technology and Biotechnology* **91**, 1452–1460.

Tran, H., You, S., Bandegharaei, A. & Chao, H. 2017 Mistakes and inconsistencies regarding adsorption of contaminants from aqueous solutions: a critical review. *Water Research* **120**, 88–116.

Ukanwa, K. S., Patchigolla, K., Sakrabani, R., Anthony, E. & Mandavgane, S. 2019 A review of chemicals to produce activated carbon from agricultural waste biomass. *Sustainability* **11**, 6204.

Wan Ngaha, W. S., Teonga, L. C. & Hanafiaha, M. A. K. M. 2011 Adsorption of dyes and heavy metal ions by chitosan composites: a review. *Carbohydrate Polymers* **83**, 1446–1456.

Xiaoxiao, J., Jiangtao, W. & Jie, B. 2009 synthesis and antimicrobial activity of the Schiff base from chitosan and citral. *Carbohydrate Research* **344**, 825–829.

Yang, H., Sheikhi, A. & Theo, G. M. V. 2016 Reusable green aerogels from crosslinked hairy nano crystalline cellulose and modified chitosan for dye removal. *Langmuir* **32** (45), 11771–11779.

Zivanovic, S., Li, J., Davidson, P. M. & Kit, K. 2007 Physical, mechanical, and antibacterial properties of chitosan/PEO blend films. *Biomacromolecules* **8**, 1505–1510.

First received 5 November 2019; accepted in revised form 23 February 2020. Available online 18 March 2020